ИНДЕКС 3649

ЕРЕВАНСКИЙ ФИЗИЧЕСКИЙ ИНСТИТУТ

Preprint YERPHI-1206(83)-89

ԵՐԵՎԱՆԻ ՖԻԶԻԿԱՅԻ ԻՆՍՏԻՏՈՒՏ
ЕРЕВАНСКИЙ ФИЗИЧЕСКИЙ ИНСТИТУТ
YEREVAN PHYSICS INSTITUTE

G.G. ARAKELYAN, A.A. GRIGORYAN, N.Ya. IVANOV

HIGH SPIN RESONANCE PRODUCTION ON π-BEAMS. A THEORETICAL ANALYSIS

ЦНИИатоминформ
EREVAN - 1989

Նախնատիպ ԵՓԻ- 1206(83)-89

Գ.Հ.ԱՌԱՔԵԼՑԱՆ, Ա.Ա.ԳՐԻԳՈՐՑԱՆ, Ն.Ցա.ԻՎԱՆՈՎ

π -ՓՆՋԵՐԻ ՄԵԾ ՍՊԻՆՈՎ ՌԵԶՈՆԱՆՍՆԵՐԻ ԾՆՄԱՆ ՓՈՐՁԱՐԱՐԱԿԱՆ ՏՎՅԱԼՆԵՐԻ ԺԱՄԱՆԱԿԱԿԻՑ ՎԻՃԱԿԸ

Կատարվել է πN -բախումներում $J \geq 2$ սպինով բոզոնային ռեզոնանսների էքսկլուզիվ ծնման փորձարարական տվյալների տեսական վերլուծություն, որոնք ընկած են ρ և f հետագծի վրա: Մոդելը հենված է պիոնների փոխանակման ռեջեացված մոտավորության և ռեզոնանսների տրոհման համար՝ ուժեղ փոխազդեցությունների քվարկ-գլյուոնային կանխատեսման վրա: Կտրվածքների ներդրումների հաշվարկը ցույց է տալիս, որ նրանք զգալիորեն չեն փոխում միապիոնային փոխանակման կանխատեսումը: Մոդելը որակապես նկարագրում է փորձի տվյալների մեծ ամբողջությունը:

Երևանի Ֆիզիկայի Ինստիտուտ
Երևան 1989

1. Introduction

As the basic sources for experimental study of characteristics of high J spin resonances there serve quasi-two-body processes of πN-collisions:

$$\pi N \to JN \tag{1.1}$$

and

$$\pi N \to J\Delta \tag{1.2}$$

Today we have considerable information on differential cross sections of these processes for resonances lying on ρ- and f-Regge trajectories, up to J=6. Production of these resonances at not very high energies is caused largely by t-channel pion exchange. Here a question arises concerning the systematical theoretical analysis of the whole set of available experimental data on processes (1.1) and (1.2) (differential and integral cross sections, density matrices) in the framework of one-pion exchange (OPE) model.

This problem was partly considered in Ref.[1]. By fitting

differential cross sections and partial probabilities of resonance decays, authors analyzed dependence of integral cross section of reaction (1.1) $\sigma_N^J(S)$ on spin J. They concluded that it is possible to self-consistently describe all experimental cross sections of high spin production in process (1.1). However Ref. [1] contains some inaccuracies (in particular, the coefficient before formula (6) as well as the cross sections in Fig.5 are twice underrated). As will be shown in the present work, the cross sections experimentally measured on a SAMB-2000 spectrometer [2] are substantially lower than the OPE model predictions (even with account of cut contributions), thereby differing from the rest of the world data on reactions (1.1) and (1.2) which are in good agreement with theoretical calculations.

The work is designed as follows. In Section 2 we give a description of the model. Section 3 is devoted to the analysis of experimental data on differential cross sections of produced mesons as well as to their comparison with theoretical predictions. Characteristic features of the model proposed are discussed: t-dependence of processes (1.1) and (1.2) cross sections, their dependence on resonance spin J and on initial energy, cut contributions. Section 4 deals with integral production cross sections and density matrices $\rho^J_{\lambda\lambda'}$ of highest states. In particular, we give predictions of the model for σ_N^J and $\rho^J_{\lambda\lambda'}$ at Batavia energies E_L = 100 and 175 GeV. In Section 5 we analyse correct choice of final states ($\pi\pi$, $K\bar{K}$, $N\bar{N}$, etc.) as a basis for most effective search for high spin resonances in these states. In Appendix we have calculated s-channel helicity amplitudes of processes $\pi N \to Jd$ (d=N, Δ) corresponding to π -exchange.

2. Description of the Model

Our proposed model to describe resonance production in processes $\pi N \to Jd$ ($d = N, \Delta$) is based on predictions of the quark-gluon picture (QGP) of strong interactions for two-body decays $J \to ab$ [3,4] and reggeized pion exchange (OPER). In one-pion approximation these reactions are described by a diagram shown in Fig.1a. The corresponding amplitude $\mathcal{M}^{\pi}_{\lambda_N \to \lambda_J \lambda_d}(s,t)$ is as follows:

$$\mathcal{M}^{\pi}_{\lambda_N \to \lambda_J \lambda_d}(s,t) = V^{\pi\pi J}_{\lambda_J} V^{N\pi d}_{\lambda_N \to \lambda_d} F_\pi(s,t) \qquad (2.1)$$

$V^{\pi\pi J}_{\lambda_J}$ represents the vertex $J \to \pi\pi$ where one of the pions is off mass shell and its invariant form is

$$V^{\pi\pi J}_{\lambda_J} = \frac{1}{2^J} G_J \varphi_{\mu_1 \dots \mu_J}(P_J, \lambda_J)(P_\pi^{\mu_1} - q^{\mu_1}) \cdots (P_\pi^{\mu_J} - q^{\mu_J}) \qquad (2.2)$$

where $\varphi_{\mu_1 \dots \mu_J}(P_J, \lambda_J)$ is a wave function of resonance with spin J and helicity λ_J . According to the boson resonance decay model [3] based on QGP of strong interactions, the decay constant G_J depends on spin J as follows:

$$G_J^2 = g_\rho^2 \frac{2^{J+1}}{S_0^{J-1}(J-1)!} \qquad (2.3)$$

where $S_0 = (\alpha'_\rho)^{-1} = 1.1\ (\mathrm{GeV/c})^2$, and $\frac{g_\rho^2}{4\pi} = 2.93$ is determined from decay $\rho \to 2\pi$.

For vertices $V^{N\pi d}_{\lambda_N \to \lambda_d}$ ($d = N$, Δ ; λ_d are the corresponding helicities) we have

$$V^{N\pi N}_{\lambda_N \to \lambda'_N} = G_{N\pi N}\, \bar{u}(P'_N, \lambda'_N)\gamma^5 u(P_N, \lambda_N)$$

$$V^{N\pi\Delta}_{\lambda_N \to \lambda_\Delta} = \frac{1}{2} G_{N\pi\Delta}\, \bar{u}_\mu(P_\Delta, \lambda_\Delta) u(P_N, \lambda_N)(P_N^\mu - q^\mu) \qquad (2.4)$$

Constants $G_{N\pi N}$ and $G_{N\pi\Delta}$ have the following values:

$$\frac{G^2_{p\pi^0 p}}{4\pi} = 14.6\ , \qquad \frac{G^2_{p\pi^+\Delta^{++}}}{4\pi} = 19\ \text{GeV}^{-2}$$

Turn now to the Green function $F_\pi(s,t)$. Nearness of pion pole to physical scattering region allows one to fix for small $|t| \approx \mu^2$ normalization of cross sections of considered processes in an absolute way. Pion off mass shell effects are taken into account by means of the form-factor $F_\pi(s,t)$ which in the OPER model is parametrized as follows:

$$F_\pi(s,t) = e^{\Lambda(t-\mu^2)}\, e^{-i\pi\alpha_\pi(t-\mu^2)/2} \times \begin{cases} \dfrac{\pi\alpha'_\pi}{2\sin\frac{\pi}{2}\alpha_\pi(t-\mu^2)}, & |t| < |t_0| \\ \dfrac{\pi\alpha'_\pi e^{R_2^2(t-t_0)}}{2\sin\frac{\pi}{2}\alpha_\pi(t_0-\mu^2)}, & |t| > |t_0| \end{cases} \qquad (2.5)$$

Here $\Lambda = R_1^2 + \alpha'_\pi \ln\frac{s}{s_0}$, $R_1^2 = 0.3\ (\text{GeV/c})^{-2}$, $R_2^2 = 2.0\ (\text{GeV/c})^{-2}$, $t_0 = -0.6\ (\text{GeV/c})^2$, $\alpha_\pi(t-\mu^2) = \alpha'_\pi \times (t-\mu^2)$, $\alpha'_\pi = 1\ (\text{GeV/c})^{-2}$. Parameters R_1^2, R_2^2 and t_0 were determined from data on differential cross sections of ρ-meson production[1].

---

[1] They turned out rather close to the values obtained in Ref. [5] from the analysis of nucleon inclusive spectra.

Thus the pion pole contribution to the differential cross sections of reactions (1.1) and (1.2) is

$$\frac{d\sigma_d^J}{dt} = \frac{1}{64\pi P_0^2 s}\ \frac{1}{2J+1} \sum_{\lambda_J,\lambda_N,\lambda_d} \left| \mathcal{M}^\pi_{\lambda_N \to \lambda_J \lambda_d}(s,t) \right|^2 = \qquad (2.6)$$

$$= \frac{1}{64\pi P_0^2 s} \left| \overline{V^{\pi\pi J}(t)} \right|^2 \left| \overline{V^{N\pi d}(t)} \right|^2 \left| F_\pi(s,t) \right|^2$$

In expression (2.6) $P_0 = Q(s, m_N^2, \mu^2)$ is 3-momentum in the c.m.s. of initial π-meson and nucleon; $Q(x,y,z) = \sqrt{(x-y-z)^2 - 4yz}\,/\,2\sqrt{x}$;

$$\left| \overline{V^{\pi^+\pi^- J^0}(t)} \right|^2 = 2 g_\rho^2 \left(\frac{4P_t^2}{s_0}\right)^J \frac{s_0 J!\, J}{(2J)!} \qquad (2.7)$$

$P_t = Q(M_J^2, \mu^2, t)$ is 3-momentum of a real and virtual pions in the rest frame of resonance J;

$$\left| \overline{V^{N\pi N}(t)} \right|^2 = -G^2_{N\pi N} t \qquad (2.8)$$

$$\left| \overline{V^{N\pi\Delta}(t)} \right|^2 = \frac{G^2_{N\pi\Delta}}{6 m_\Delta^2} \left[(m_\Delta - m_N)^2 - t\right]\left[(m_\Delta + m_N)^2 - t\right]^2$$

Since experimentally the resonances are observed in concrete channels, then to compare our predictions with experimental data it is necessary to take account of the decay factor connected with the decay mode to this channel (see diagram in Fig.1c). Its account effectively is reduced to multiplication of theoretical cross sections of resonance production by probability of decay channel. For partial decay widths we used QGP predictions presented in Table 1.

It should be noted that theoretical cross sections (as well as predictions on decay widths) for high spins are rather sensitive to the resonance mass M_J. According to (2.7), they behave as $P_t^{2J} \approx M_J^{2J}$. Therefore, in Table 1 we give values of masses at which partial widths and cross sections of resonance production were calculated.

Further on, the cross sections are multiplied by the correction factor $a(\Gamma_J)$ connected with experimental cutoff imposed on invariant mass of decay products. On the assumption of the Breit-Wigner form of distribution the factor $a(\Gamma_J)$ is

$$a(\Gamma_J) = \frac{1}{\pi}\left(\operatorname{arctg}\frac{M_B^2 - M_J^2}{M_J\,\Gamma_J} - \operatorname{arctg}\frac{M_J^2 - M_H^2}{M_J\,\Gamma_J}\right),$$

where M_B and M_H are cutoff upper and lower boundaries, and Γ_J is total width of resonance.

Now we'd like to discuss the question of pion-pomeron cut contribution (see Fig.1b). When calculating it, we used formalism of s-channel helicity amplitudes. The helicity amplitude corresponding to pole exchange is determined by projection of invariant form (2.1) on states with given helicity in the infinite momentum frame (see Appendix). The expression that describes contribution of $\pi\mathbb{P}$ -cut to the s-channel helicity amplitude is of the form [6] :

$$\mathcal{A}^{\pi\mathbb{P}}_{\lambda_N \to \lambda_J \lambda_d}(s, q_\perp) = \frac{i}{8\pi^2 s}\sum_{\lambda_{\pi^*},\lambda_{N^*}}\int d^2K_\perp \times \tag{2.9}$$

$$\times\, \mathcal{A}^{\mathbb{P}}_{\lambda_N \to \lambda_{\pi^*}\lambda_{N^*}}(s, \vec{K}'_\perp)\, \mathcal{A}^{\pi}_{\lambda_{\pi^*}\lambda_{N^*} \to \lambda_J \lambda_d}(s, \vec{K}_\perp)$$

In formula (2.9) π^* and N^* are intermediate states; $\vec{K}'_\perp = \vec{q}_\perp - \vec{K}_\perp$. Let's assume that among the intermediate states

the pole one, ($\pi + N$), dominates. Then the right-hand side of formula (2.9) will contain amplitudes of elastic πN -scattering, $\mathcal{A}^{\mathbb{P}}_{\lambda_N \to \lambda'_N}(s, \vec{K}_\perp)$, corresponding to single-pomeron exchange, and amplitude (A.5) of one-pion exchange.[2)]

Under this assumption, the major contribution is made by the cuts corresponding to the transition in vertex $N\mathbb{P}N$ with conserved helicity. A simple analysis shows that the contribution to the cross section of cuts corresponding to spin-flip transition in vertex $N\mathbb{P}N$ is negligibly small. This is due to both the smallness of spin-flip residue of vacuum pole and the numerical smallness of resultant coefficients.

For the spin-nonflip amplitude $\mathcal{A}^{\mathbb{P}}_{\lambda_N \to \lambda_N}$ we used the following parametrization:

$$\mathcal{A}^{\mathbb{P}}_{\lambda_N \to \lambda_N}(s, \vec{K}_\perp) = i g^{\mathbb{P}} \frac{s}{\bar{s}} e^{-\vec{K}_\perp^2 b_{\mathbb{P}}} \tag{2.10}$$

where $\bar{s} = 1\ \text{GeV}^2$.

Using for contribution (2.10) to the elastic πN -scattering the optical theorem we obtain:

$$\mathcal{A}^{\mathbb{P}}_{\lambda_N \to \lambda_N}(s, \vec{K}_\perp) = i s \sigma^{\pi N}_{tot}\, e^{-\vec{K}_\perp^2 b_{\mathbb{P}}} \tag{2.11}$$

From the analysis of total cross sections and slopes of πN -processes we have the following values:

$$\sigma^{\pi N}_{tot} = 25\ \text{mb}\ ; \qquad b_{\mathbb{P}} = 4\ (\text{GeV/c})^2$$

---

2) It may be that contribution of inelastic states is not small in the case of highest spins J; however the analysis of this question is beyond the scope of our paper.

Return to formula (2.9). After integration over angle ($\int d^2\kappa_\perp = \int_0^{2\pi} d\varphi \int_0^\infty \kappa_\perp d\kappa_\perp$) we obtain:

$$\mathcal{M}^{\pi P}_{\lambda_N \to \lambda_y \lambda_d}(s, q_\perp) = -\frac{\sigma^{\pi N}_{tot}}{4\pi} e^{-b_P q_\perp^2} \int_0^\infty d\kappa_\perp \kappa_\perp e^{-b_P \kappa_\perp^2} \times \tag{2.12}$$

$$\times I_n(2b_P q_\perp \kappa_\perp)\, \mathcal{M}^{\pi}_{\lambda_N \to \lambda_y \lambda_d}(s, \kappa_\perp)$$

Here $I_n(x)$ is a modified Bessel function; $n = |\lambda_y - \lambda_d + \lambda_d|$.

3. Differential Cross Sections

Thus the model proposed allows one to take account of contributions of pion pole and πP -cut to $\pi N \to Jd$ ($d = N, \Delta$) processes. Before starting a comparison between experimental data and theoretical predictions, let us consider some typical features of our model.

In the region of small values of transferred momenta in the considered reactions the one-pion exchange is dominant, which is due to nearness of the pion pole to the physical region of scattering. Amplitudes of processes (1.1) and (1.2) at small t behave as

$$\frac{\sqrt{t}}{t-\mu^2} \tag{3.1}$$

and

$$\frac{const}{t-\mu^2} \tag{3.2}$$

respectively. So long as amplitudes (2.12) have no pole behavior, the account of πP -cut does not essentially affect predictions of one-pion approximation. The cut contribution is negligibly small in differential cross section maxima which coincide

with maxima of expressions (3.1) ($t \approx -\mu^2$) and (3.2) ($t' \approx 0$) and slowly increases with growing $|t|$. Our calculations show that the fraction of cut contributions to cross sections is weakly dependent on spin J. We shall not dwell in detail on ρ (770)-meson production experiments because a large number of works are devoted to their analysis within the one-pion exchange model. We'll present only some data that demonstrate the validity region of the model.

Figs. 2a and 2b show differential cross sections of ρ^0 -meson production in reactions (1.1) and (1.2). At not high energies (up to P_L = 17 GeV/c) one can observe a good description in a large range of transferred momenta. Of great interest are the cross sections measured at high energies (100 and 175 GeV). As one can see from Fig. 2b, even at these energies the pion exchange is dominant in the region of small values of transferred momenta (up to $\sqrt{-t}$ = 0.3 GeV/c). The deviation of predictions of the model from experimental data at $\sqrt{-t} > 0.3$ GeV/c stands for the fact that at these energies the contribution of Regge poles with natural parity becomes significant.

In Fig.2, to illustrate relative contributions of the pole and cut, the contribution of pole amplitude (2.1) is separated. In order not to encumber the figures, we'll give for resonances with $J \geqslant 2$ only the contribution of total amplitude with cut (2.12).

Comparison of theoretical predictions with experimental data on production of $f_2(1270)$-meson (J=2) is presented in Fig.3. Except for the experiment [2] at P_L = 38 GeV/c one can

observe a good description of data in a large (up to -1 $(GeV/c)^2$) range of t.

Processes with production of $\rho_3(1690)$ (j=3) resonance are studied in less detail experimentally. Fig.4a presents predictions for reaction $\pi^- p \to \rho_3(1690) n$ at $P_L = 7$ and 8 GeV/c. Ibidem we present comparison with experimental data for process $\pi^+ p \to \rho_3(1690)\Delta^{++}$ at $P_L = 18.5$ GeV/c. In both cases the theoretical curve keeps within experimental errors, although, owing to large values of the latters, it is hard to judge of the accuracy of predictions.

As for the resonances with J=4, here experimental information on differential cross sections of their production is fairly scarce. The available data for $f_4(2050)$- and $\Gamma(2510)$-mesons (J=4 and 6, respectively) at $P_L = 38$ GeV/c are given in Fig.4b. One can see that these data obtained in the experiment [2] are several times less than the model predictions.

Thus the simple model with a universal J spin-independent pion form-factor (2.5) describes rather successfully a large set of differential cross sections of resonance production. The exception here are the data on f_2-, f_4- and Γ-mesons obtained at $P_L = 38$ GeV/c on a GAMS-2000 spectrometer [2] that are considerably lower than theoretical predictions. The attempts to attain an agreement between theoretical predictions and results of [2] by means of enhancing cut contribution (this would have corresponded to anomalously large contribution to (2.9) from other intermediate states, $\pi^* + N^*$) lead to a disagreement with other world data. Besides, recently in Ref. [7] data were published on f_2- and f_4- meson production cross sections

at the same energy 38 GeV. These data are higher than those reported in Ref. [2] and are in better agreement with theoretical predictions (see Fig.7a).

4. Integral Cross Sections. Density Matrices.

Predictions of the model for integral cross sections $\sigma_N^J(S)$ of resonance production in processes (1.1) up to 50 GeV are presented in Fig.5a. For convenience in comparison, all considered cross sections (both theoretical and experimental[3]) are reduced to the value corresponding to integration region $0 < |t'| < 0.2$ $(GeV/c)^2$, i.e. $\sigma_N^J(S) = \int_0^{0.2} \frac{d\sigma(s,t')}{dt'} d|t'|$. In this region the cut contribution is not large, it does not exceed 15% in all cases considered.

Our predictions for integral cross sections of f_2 -meson with a good accuracy have a behavior $\sigma_N^{f_2}(S) \sim P_L^{-2}$. At sufficiently high energies the curves for $J > 2$ behave similarly. As can be seen from Fig.5a, the available experimental data (except [2]) are in reasonable agreement with theoretical predictions.

---

3) The cross section data were taken from the following papers:
for J=2 - [8] ($P_L = 4.5$ GeV/c), [9] (6), [10] (8), [11] (12,15), [12] (16), [13] (17), [2,7] (38);
J=3 - [9] ($P_L = 6$ GeV/c), [14] (7), [10] (8);
J=4 - [15] ($P_L = 10$ GeV/c), [16] (18.4), [2,7] (38);
J=6 - [2] ($P_L = 38$ GeV/c).

In determining the quantities $\sigma_N^{f_4}(S)$ from data [7,15,16] we used the table value $Br(f_4 \to K\bar{K}) = 0.7\ ^{+0.4}_{-0.2}$ %. The QGP predictions for $f_4 \to K\bar{K}$ decay (see Table 1) are somewhat higher.

To elucidate the role of pion exchange at high energies, the measurements of cross sections of high spin production at energies of Batavia experiment [17] are highly interesting. Fig.5b shows our predictions for these cross sections (up to J=6) at E_L = 100 and 175 GeV. As was mentioned in the previous section, the data of [17] on ρ -meson production restrict the validity region of the π -meson approach at these energies to values $\sqrt{-t'}$ = 0.3 GeV/c. Therefore, our predictions in Fig.5b have narrower boundaries of intergration: $0 < |t'| < 0.1$ (GeV/c)^2.

Turn now to density matrices $\rho^J_{\lambda\lambda'}$ of high spins. Experimental data are available only on density matrix of f-meson [11,18] being, we should note, not model-independent. The elements $\rho^2_{\lambda\lambda'}$ were calculated from data on angular distribution of resonance decay products under some assumptions on the nature of exchange amplitudes.

In Fig.6a,b we present a comparison between data of those works and predictions of our model. The density matrix elements are given in the s-channel helicity frame. Reasonable agreement between predictions and experiment stands for the fact that the helicity amplitudes (2.12) and (A.2) (see the Appendix) have a correct t-behavior.

To illustrate the $\pi\mathbb{P}$ -cut contribution, we also present curves corresponding to contributions of pole amplitudes. One can see that account of cut affects weakly the predictions being most sensible in the region of superlow values of transferred momenta $|t| < 0.01$ (GeV/c)^2. In all cases the nature of t-dependence of quantities $\rho^J_{\lambda\lambda'}$ depends weakly on

initial energy.

Changes in s-channel density matrices that are due to growing resonance spin are demonstrated in Fig.6c. Here we give predictions for J=2 and 6 at E_L = 100 GeV. Predictions for J=3,4 and 5 lie in the narrow interval between curves given in Fig.6c. As for contributions of amplitudes with s-channel helicity $|\lambda_3| \geq 2$, the calculations show that they are negligibly small.

5. In What Systems the High-Spin Resonances Should Be Searched for?

Now we'd like to dwell at greater length on experimental data on ρ- , f_2- and ρ_3 -meson production at 17 GeV [13] . The $\pi^+\pi^-$ system produced on a π^--beam was analyzed experimentally. Fig.7a shows that experimental data prevail over our predictions, the discrepancy being enhanced with increasing mass of the $\pi^+\pi^-$ system. However one can readily be convinced that this discrepancy is seeming. The point is that the Ref. [13] presents data on $\pi^+\pi^-$ system production in the mass regions corresponding to ρ^- , f_2^- and ρ_3^- mesons without separation of the background under resonances. A simple duality-based analysis shows that in the $\pi^+\pi^-$ system produced on $\pi^\pm$ -beams the background under resonances may be large and must grow with increasing mass $M_{\pi^+\pi^-}$. Indeed, consider the amplitude $\pi^+\pi^- \to \pi^+\pi^-$ in the upper block of diagram 1c. Following two-component Harari-Freund duality, secondary Regge trajectories exchanges in t-channel correspond to resonance contribution in direct channel (see Fig.8a). and background under resonances is dual

to contribution of vacuum nonplanar singularity (see Fig.8b). Insofar as to seconadry Regge-trajectories there corresponds the behavior $(M^2_{\pi^+\pi^-})^{\alpha_\rho(0)\approx 0.5}$, and to vacuum singularity - $(M^2_{\pi^+\pi^-})^{\alpha_P(0)\approx 1}$, then with increasing the $\pi^+\pi^-$ system mass the signal-background ratio falls off as $(M^2_{\pi^+\pi^-})^{-0.5}$.

Thus the resonances produced on $\pi^\pm$ beams should be searched for in the systems for which the diagram of Fig.8b is absent. To those systems there refer, for instance, $\pi^\circ\pi^\circ$, $K\bar{K}$, $N\bar{N}$. If we isolate in them states with the given spin J, then according to the dual Veneziano model the corresponding partial amplitude is zero up to the mass of the resonance lying on the rightmost Regge trajectory. For example, a signal in partial amplitudes with J=2 and J=4 must appear beginning with the $f_2(1270)$ and $f_4(2050)$ resonance masses, respectively. Such a behavior of partial amplitudes actually is observed in the system $K^\circ_S K^\circ_S$ in experiments [7] [4].

Similarly, in order to effectively search for strange high-spin resonances produced on $K^+(K^-)$ beams, one should study the systems $K^\circ\pi(\bar{K}^\circ\pi)$. In $K^+\pi(K^-\pi)$ channels a large background is expected. The same background is to be observed in the $p\bar{p}$ system too, produced in experiments on the LEAR at CERN.

The separation of the resonance signal from the background in experimental data [13] on $\pi^+\pi^-$ production in the region of $f_2(1270)$-meson was realized in Ref. [19]. Fig.7b demonstrates a good agreement between our predictions and obtained data.

4) V.N. Nozdrachev, private communication.

Conclusion

Thus the model based on reggeized one-pion exchange and QGP predictions for resonance decays allows to describe the large set of experimental data on exclusive production of ρ - and f-trajectory resonances on π -beams.

The main conclusions resultant from the above analysis are as follows:

i) the pion exchange has a universal nature, i.e. the form-factor that describes the off mass shell π -meson is spin-independent. Note that our used form-factor (2.5) describes correctly inclusive spectra of nucleons [5] and $\rho(770)$-meson (to be published), i.e. here too one can observe pion exchange universality;

ii) at small $|t|$ ($\sqrt{-t} \leq 0.3$ GeV/c) pion exchange dominates up to the energy of 175 GeV (measurements at high energies are absent). At not very high energies OPER describes experimental data in a sufficiently large region of transferred momenta ($|t| \leq 1$ (GeV/c)^2);

iii) account of pion-pomeron cuts does not essentially affect predictions of one-pion approximation[5].

To enlarge the applicability region of the proposed model, it is interesting to analyze exclusive and inclusive production of kaon resonances in K -beam experiments as well as to include into the scheme the contributions of natural Regge poles in

5) We do not discuss here a very narrow region of variable t ($|t| \ll \mu^2$) where contribution of cuts not conserving parity can be crucial.

order to describe experimental data in a wide interval of transferred momenta at high energies.

On the other hand, in the experimental situation concerning the analysis of high spin production there exists a fairly large number of ambiguities, so in independent experiments it is necessary to solve such problems as:

I. Measurements at very high energies ($E_L \geq 200$ GeV) of exclusive cross sections of production of ρ-meson as well as the highest states.

II. Analysis of inclusive spectra of spin $J \geq 2$ states produced on π - and K-beams.

III. Accurate measurements of density matrix elements of produced resonances.

IV. Simultaneous study of characteristics of spin J resonances in different final states ($\pi\pi$, $K\bar{K}$, $N\bar{N}$, etc.).

APPENDIX

Firstly, we calculate s-channel helicity amplitudes corresponding to one-pion exchange. To do that, we project expression (21) on helicity states in the frame where the incident pion has a large momentum, i.e. in the infinite momentum frame (IMF). Obviously, the IMF in a natural way corresponds to the s-channel scattering frame at high energies.

To calculate helicity projections of vertex (2.2), we make use of the wave function $\varphi_{\mu_1 \dots \mu_J}(P_J, \lambda_J)$ of state with spin J and helicity λ_J in Rarita-Schwinger formalism:

$$\varphi_{\mu_1 \dots \mu_J}(P_J, \lambda_J) = \sqrt{\frac{2^J (J+\lambda_J)!(J-\lambda_J)!}{(2J)!}} \sum_{\substack{\beta_1 \dots \beta_J \\ \Sigma \beta_i = \lambda_J}} \left[(1+\beta_1)!(1-\beta_1)! \dots \right. \tag{A.1}$$

$$\left. \dots (1+\beta_J)!(1-\beta_J)! \right]^{-1/2} \xi_{\mu_1}(P_J, \beta_1) \dots \xi_{\mu_J}(P_J, \beta_J)$$

where vector $\xi_{\mu_i}(P_J, \beta_i)$ describes a state with spin 1 and helicity β_i .

With the use of (A.1) we come to the following representation for helicity transitions (2.2) in IMF:

$$V^{\pi\pi J}_{\lambda_J}(\vec{q}_\perp) = G_J \sqrt{\frac{2^J (J+\lambda_J)!(J-\lambda_J)!}{(2J)!}}\, e^{-i\varphi\lambda_J} \left(\frac{a(\mathrm{sign}\,\lambda_J)}{\sqrt{2}} \right)^{|\lambda_J|} \times$$

$$\times \sum_{n=0}^{m} C^J_{|\lambda_J|+2n} C^{|\lambda_J|+2n}_n (a(0))^{J-|\lambda_J|-2n} \left(\frac{a(1)a(-1)}{2} \right)^n \equiv \tag{A.2}$$

$$\equiv V^{\pi\pi J}_{\lambda_J}(q_\perp)\, e^{-i\varphi\lambda_J}$$

In formula (A.2) $C_q^p = \frac{p!}{q!(p-q)!}$, summation over integer n goes up to m satisfying the condition:

$$\frac{J-|\lambda_J|-1}{2} \leqslant m \leqslant \frac{J-|\lambda_J|}{2}$$

$a(\lambda) = \xi^*_\mu W^\mu_q e^{i\varphi\lambda}$, φ is the angle between the x axis and $\vec{q}_\perp$ (the incident pion momentum is directed along the z axis).

In the IMF we have

$$a(\pm 1) = \mp \frac{q_\perp}{\sqrt{2}}, \qquad a(0) = \sqrt{P_t^2 - \vec{q}_\perp^{\,2}} \tag{A.3}$$

Projections of vertices $V^{N\pi d}_{\lambda_N \to \lambda_d}$ on helicity states in the IMF (for these vertices the IMF momentum coincides with initial nucleon momentum in the c.m.s. of the reaction) are as follows:

$$V^{N\pi d}_{1/2\to\lambda_d}(\vec{q}_\perp) = V^{N\pi d}_{1/2\to\lambda_d}(q_\perp)\, e^{-i\varphi(1/2-\lambda_d)}$$

where

$$V^{N\pi N}_{1/2\ 1/2} = 0$$

$$V^{N\pi N}_{1/2\ -1/2} = q_\perp G_{N\pi N}$$

$$V^{N\pi\Delta}_{1/2\ 1/2} = -\frac{(m_\Delta+m_N)^2(m_\Delta-m_N)-q_\perp^2(2m_\Delta+m_N)}{\sqrt{6}\,m_\Delta} G_{N\pi\Delta} \tag{A.4}$$

$$V^{N\pi\Delta}_{1/2\ -1/2} = \frac{(m_\Delta+m_N)(2m_\Delta-m_N)-q_\perp^2}{\sqrt{6}\,m_\Delta} q_\perp G_{N\pi\Delta}$$

$$V^{N\pi\Delta}_{1/2\ 3/2} = -\frac{(m_\Delta+m_N)}{\sqrt{2}} q_\perp G_{N\pi\Delta}$$

$$V^{N\pi\Delta}_{1/2\ -3/2} = -\frac{1}{\sqrt{2}} q_\perp^2 G_{N\pi\Delta}$$

Thus the expression for the contribution of pion pole to the s-channel helicity amplitude describing processes (1.1) and (1.2) at high energies is of the form:

$$\mathcal{M}^{\pi}_{1/2\to\lambda_J\lambda_d}(s,\vec{q}_\perp) = \mathcal{M}^{\pi}_{1/2\to\lambda_J\lambda_d}(s,q_\perp)\, e^{i\varphi(-1/2-\lambda_J+\lambda_d)} \tag{A.5}$$

$$\mathcal{M}^{\pi}_{1/2\to\lambda_J\lambda_d}(s,q_\perp) = V^{\pi\pi J}_{\lambda_J}(q_\perp)\, V^{N\pi d}_{1/2\to\lambda_d}(q_\perp)\, F_\pi(s,t)$$

with $V^{\pi\pi J}_{\lambda_J}(q_\perp)$ and $V^{N\pi d}_{1/2\to\lambda_d}(q_\perp)$ defined in (A.2) and (A.4).

Note, that we keep the variable $t = t_{min} - \vec{q}_\perp^{\,2}$ in the Green function $F_\pi(s,t)$ because at not very large S and large masses M_J the effects connected with t_{min} are essential.

Table . QGP predictions for widths of resonance decays to two pseudoscalars

Resonance	J^P	M_J(MeV)	$\Gamma_{\pi^+\pi^-}$(MeV)	$\Gamma_{K\bar{K}}$ (MeV)
$f_2(1270)$	2^+	1274	83 ± 3	3.8 ± 0.3
$\rho_3(1690)$	3^-	1691	54 ± 3	4.7 ± 0.4
$f_4(2050)$	4^+	2027	32 ± 4	3 ± 0.4
J_5	5^-	2240	20 ± 5	1.6 ± 0.2
$r(2510)$	6^+	2510	14.5 ± 2	0.8 ± 0.1

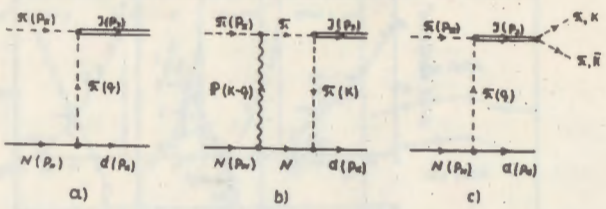

Fig. 1

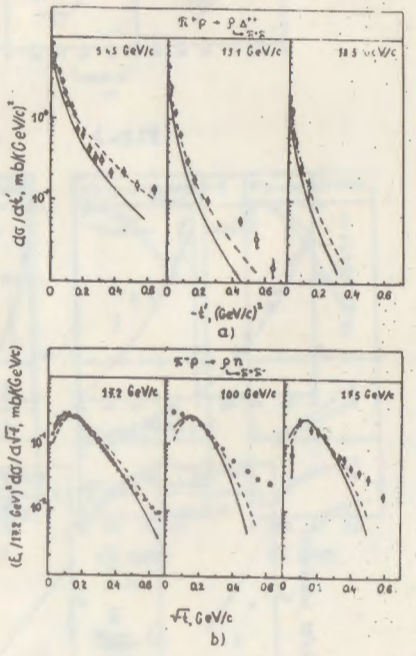

Fig. 2

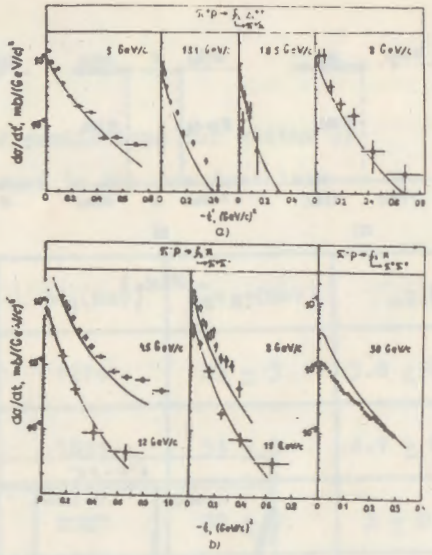

Fig.3

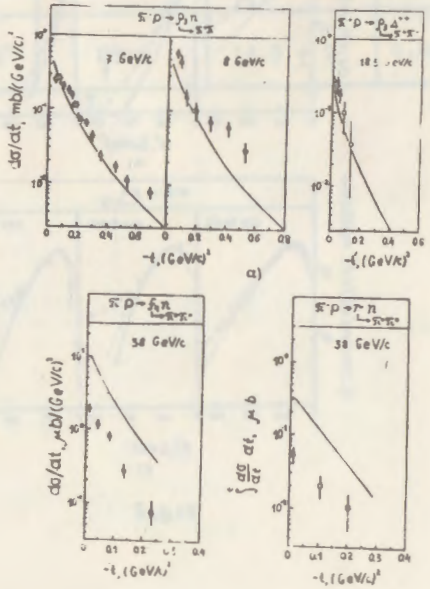

Fig.4

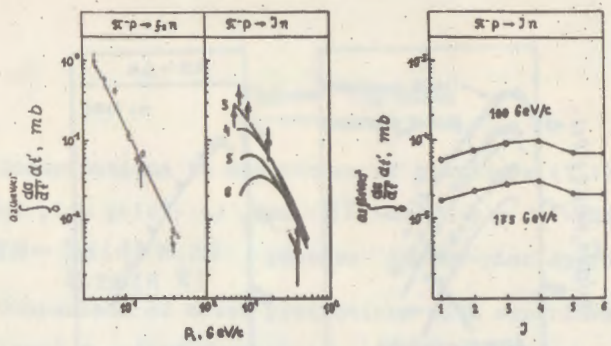

Fig.5

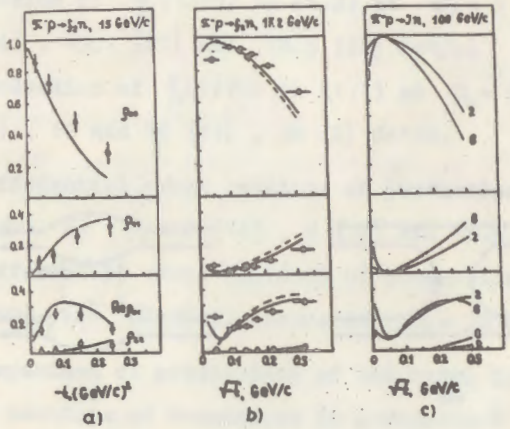

Fig.6

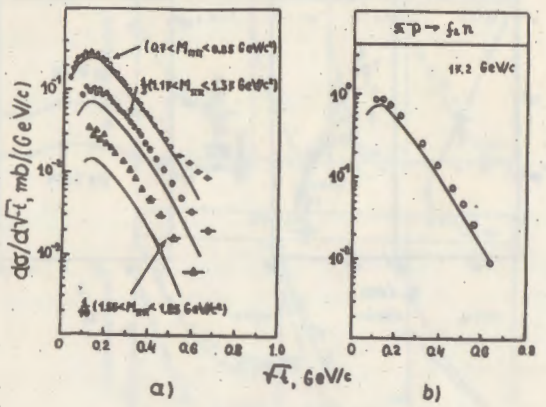

Fig.7

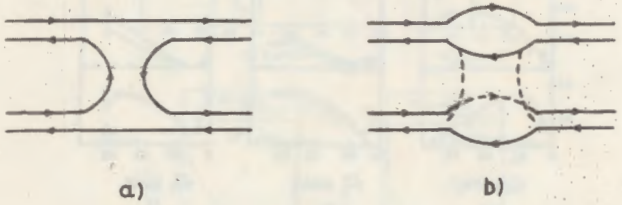

Fig.8

Figure Captions

Fig.1. Contributions to amplitudes of processes (1.1) and (1.2) of pion pole - a) and πP -cut - b); c) - diagram of $\pi N \to Jd\,(d = N, \Delta)$, $J \to 2\pi\,(K\bar{K})$ process in one-pion approximation.

Fig.2. Comparison of model predictions with experiment (solid line) for differential cross sections of processes $\pi^+ p \to \rho^0 \Delta^{++}$ (data of Refs: [20] (p_L = 5.45 GeV/c), [21] (13.1 GeV/c), [22] (18.5 GeV/c)) and $\pi^- p \to \rho^0 n$ (data of Refs [13] (17.2 GeV/c) and [17] (100,175 GeV/C)). Dots - pion pole contribution.

Fig.3. a) Comparison with experiment of predictions for production of $f_2(1270)$ in (1.2) at p_L = 5 [23] 8 [24] , 13.1 [21] and 18.5 [22] GeV/c;
b) production of $f_2(1270)$ in (1.1) at p_L = 4.5 [8] , 8 [10] , 12 and 15 [11] , 38 [2] GeV/c.

Fig.4. a) Differential cross sections of production of $\rho_3(1690)$ at p_L = 7 [14] , 8 [10] and 18.5 [22] GeV/c;
b) differential cross sections of production of $f_4(2050)$- and $r(2510)$-mesons at p_L = 38 GeV/c [2] .

Fig.5. a) Comparison of predictions of the model for integral cross sections of resonances in processes $\pi^- p \to Jn$ with experimental data; o - data on f_2 -meson, Δ - on ρ_3 -meson, $\square$ - on f_4 -meson;
b) predictions for integral cross sections at p_L = 100 and 175 GeV/c depending on spin J.

Fig.6. a), b) Comparison of predictions of the model for density matrix of $f_2(1270)$-meson in process (1,1) with data of Refs [11] (P_L = 15 GeV/c) and [13,18] (17.2 GeV/c); dots - π-meson contribution; c) predictions for density matrices of resonances with spin J=2 and 6 at P_L = 100 GeV/c. Predictions for J=3,4 and 5 lie between curves given in Fig.6c. All predictions are given in the s-channel helicity frame.

Fig.7. a) Differential cross sections of process $\pi^- p \to \pi^- \pi^+ r$ in mass regions of $\rho\,(0.7 < M_{\pi\pi} < 0.85\ \mathrm{GeV/c^2})$, $f_2(1.17 < M_{\pi\pi} < 1.37\ \mathrm{GeV/c^2})$ and $\rho_3(1.55 < M_{\pi\pi} < 1.85\ \mathrm{GeV/c^2})$ [13]; b) comparison of model predictions with experimental data on f_2-meson production after separation of background.

Fig.8. Contributions to $\pi\pi$-scattering amplitude of planar - a) and vacuum - b) diagrams.

REFERENCES

1. Gershtein S.S., Grudtsin S.N. Yad.Fiz., 1983, V.37, P.1563.
2. Binon F. et al. Lett.Nuovo Cim., 1984, V.39, P.41.
3. Kaidalov A.B., Volkovitsky P.E. Yad.Fiz.,1982,V.35,P.1556.
4. Grigoryan A.A., Ivanov N.Ya. Yad.Fiz., 1986, V.43, P.693.
5. Arakelyan G.G., Grigoryan A.A. Yad.Fiz., 1982, V.36, P.211.
6. Kaidalov A.B., Karnakov B.M. Yad.Fiz., 1970, V.11, P.216.
7. Bolonkin B.V. et al. Nucl.Phys., 1988, V.B309, P.426.
8. Holloway L.E. et al. Phys.Rev., 1974, V.B9, P.1161.
9. Engler A. et al. Phys.Rev., 1974, V.D10, P.2070.
10. Poirier J.A. et al. Phys.Rev., 1967, V.163, P.1462.
11. Alexander G. et al. Nucl.Phys., 1977, V.B131, P.365.
12. Bartke J. et al. Nucl.Phys., 1976, V.B107, P.93.
13. Grayer G. et al. Nucl.Phys., 1974, V.B75, P.189.
14. Matthews J. et al. Nucl.Phys., 1971, V.B33, P.1.
15. Evangelista C. et al. Nucl.Phys., 1979, V.B154, P.381.
16. Blum W. et al. Phys.Lett., 1975, V.B57, P.403.
17. Bromberg C. et al. Phys.Rev., 1984, V.D29, P.588.
18. Irving A.C., Michael C. Nucl.Phys., 1974, V.B82, P.282.
19. Martin A.D. CERN preprint TH.1741, 1973.
20. Bloodworth I.J. et al. Nucl.Phys., 1971, V.B35, P.79.
21. Gaidos J.A. et al. Phys.Rev., 1970, V.D1, P.3190; Nucl.Phys., 1971, V.B26, P.225.
22. Biswas N.N. et al. Phys.Rev., 1970, V.D2, P.2529.
23. Pols C.L. et al. Nucl. Phys., 1970, V.B25, P.109.
24. Deutschman M. et al. Phys.Lett., 1965, V.19, P.608.

The manuscript was received 31 October 1989

Г.Г.АРАКЕЛЯН, А.А.ГРИГОРЯН, Н.Я.ИВАНОВ
СОВРЕМЕННЫЙ СТАТУС ЭКСПЕРИМЕНТАЛЬНЫХ ДАННЫХ ПО РОЖДЕНИЮ
РЕЗОНАНСОВ С ВЫСОКИМ СПИНОМ НА Я - ПУЧКАХ
(на английском языке, перевод З.Н.Асланян)
Редактор Л.П.Мукаян
Технический редактор А.С.Абрамян

Подписано в печать 26/XII-89г. ВФ-II402 Формат 60x84/I6
Офсетная печать.Уч.изд.л.I,0 Тираж 299 экз. Ц. I5 к.
Зак.тип.№ I969 Индекс 3649

Отпечатано в Ереванском физическом институте
Ереван 36, ул.Братьев Алиханян,2

The address for requests:
Information Department
Yerevan Physics Institute
Alikhanian Brothers 2,
Yrevan, 375036
Armenia, USSR